Eur Biophys J (2002) 31: 428–437
DOI 10.1007/s00249-002-0233-3

ARTICLE

Oleg Konovalov · Igor Myagkov · Bernd Struth
Karl Lohner

Lipid discrimination in phospholipid monolayers by the antimicrobial frog skin peptide PGLa. A synchrotron X-ray grazing incidence and reflectivity study

Received: 31 October 2001 / Revised: 4 April 2002 / Accepted: 8 April 2002 / Published online: 28 June 2002

Abstract We present a first study using synchrotron grazing incidence diffraction and X-ray reflectivity measurements on mixed phospholipid/peptide monolayers at the air/water interface. The thermodynamic properties of the pure and mixed monolayers were characterized using the classical film balance technique. Surface pressure/potential-area isotherms showed that the antimicrobial frog skin peptide PGLa formed a very stable monolayer with two PGLa molecules per kinetic unit and a collapse pressure of ~22 mN/m. X-ray grazing incidence diffraction indicated that the peptide-dimer formation did not lead to self-aggregation with subsequent crystallite formation. However, the scattering length density profiles derived from X-ray reflectivity measurements yield information on the PGLa monolayer that protrudes into the air phase by about 0.8 nm, suggesting that the peptide is aligned parallel to the air/water interface. The monolayers, composed of disaturated phosphatidylcholines or phosphatidylglycerols, were stable up to 60 mN/m and exhibited a first-order transition from a liquid-expanded to a liquid-condensed state around 10 mN/m. Structural details of the phospholipid monolayers in the presence and absence of PGLa were obtained from synchrotron experiments. Thereby, the X-ray data of distearoylphosphatidylcholine/PGLa can be analyzed by being composed of the individual components, while the peptide strongly perturbed the lipid acyl chain order of distearoylphosphatidylglycerol. These results are in agreement that PGLa mixes at a molecular level with negatively charged lipids, but forms separate islands in zwitterionic phosphatidylcholine monolayers and demonstrates that antimicrobial peptides can discriminate between the major phospholipid components of bacterial and mammalian cytoplasmic membranes.

Keywords X-ray diffraction · Monolayer · Antimicrobial peptides · Lipid-peptide interaction · Lipid specificity

Abbreviations *DPPC*, *DSPC*: dipalmitoyl-, distearoylphosphatidylcholine · *DPPG*, *DSPG*: dipalmitoyl-, distearoylphosphatidylglycerol · *GID*: grazing incidence X-ray diffraction · *PC*: phosphatidylcholine · *PE*: phosphatidylethanolamine · *PG*: phosphatidylglycerol · *PGLa*: peptidyl-glycyl-leucine-carboxamide · *PSD*: position-sensitive detector · *SLD*: scattering length density · *SM*: sphingomyelin · *XR*: X-ray reflectivity

O. Konovalov (✉) · B. Struth
European Synchrotron Radiation Facility,
B.P. 220, 38043 Grenoble Cedex 9, France
E-mail: konovalo@esrf.fr
Fax: +33-4-76882160

O. Konovalov
UMR 5819 (CEA-CNRS-Universite J. Fourier),
17 Rue des Martyrs, 38054 Grenoble Cedex 9, France

O. Konovalov
Institute of Crystallography, Russian Academy of Sciences,
117333 Moscow, Russia

I. Myagkov
Research Institute for Physical Problems, Zelenograd, Russia

K. Lohner
Institut für Biophysik und Röntgenstrukturforschung,
Österreichische Akademie der Wissenschaften,
Schmiedlstrasse 6, 8042 Graz, Austria

Introduction

Multicellular organisms must contend with invaders such as microbes and, thus, active systems of defense have evolved in nature. In plants and animals, antimicrobial peptides, encoded by genes, represent an important part of host defense (Ganz and Lehrer 2001). In higher animals they are particularly abundant on epithelial surfaces as well as in the storage granules of phagocytic cells and consist mostly of 15–40 amino acid residues. These peptides are characterized by a positive net charge and by an amphipathic character. Antimicrobial peptides are low in cost in terms of time, information and production of energy (Boman 1991), which

is important for an effective defense at an early phase of initial infection and is in contrast to the relatively slow process of antibody-mediated specific antigen recognition. To date, several hundred different peptides, displaying a broad spectrum of antimicrobial activity, have been characterized (Tossi et al. 2000). Recently, interest in this research area has grown since antimicrobial peptides are considered as novel antibiotics which are urgently needed because of the dramatically increased number of bacterial strains that are resistant to conventional antibiotics (Davies 1996; Lohner and Staudegger 2001).

The antimicrobial activity of these peptides does not seem to be related to specific receptors, but they rather act by perturbing the barrier function of cell membranes, although alternative mechanisms such as binding to bacterial DNA after translocation across the membrane may exist (Lohner 2001). Nevertheless, independent of the molecular mechanism of killing, the cell membrane plays an important role in recognition and/or mediation of the biological activity of antimicrobial peptides. Studying the lytic activity of membrane-active peptides has revealed that many of them exhibit a high specificity towards distinct target membranes (Lohner and Epand 1997). In order to understand the molecular basis of the specific interaction of antimicrobial peptides with bacterial membranes, it is important to consider the membrane architecture of eukaryotic and prokaryotic cell membranes, which differ markedly in their complexity and lipid composition. Phosphatidylcholine (PC) and sphingomyelin (SM) are the dominant phospholipid components of the outer leaflet of eukaryotic membranes such as erythrocytes, while the prokaryotic membrane has a high content of negatively charged phospholipids and phosphatidylethanolamine (PE) (Lohner 2001 and references therein). A number of antimicrobial peptides have been shown to interact preferentially with negatively charged phospholipids, as can be expected from their cationic nature. For example, the β-sheet peptides such as human defensin (White et al. 1995; Lohner et al. 1997), protegrin-1 from porcine leukocytes (Latal et al. 1996) or tachyplesin from horseshoe crab (Nakamura et al. 1988), as well as the α-helical peptides magainin (Matsuzaki et al. 1997) and peptidyl-glycyl-leucine-carboxamide (PGLa; Latal et al. 1997), isolated from frog skin of the South African clawed frog, *Xenopus laevis*, do not affect markedly the thermotropic phase behavior of liposomes composed of choline phospholipids. However, these peptides interact preferentially with liposomes of phosphatidylglycerol (PG). Data from differential scanning calorimetry and X-ray diffraction suggest that PGLa, the focus of this study, induces lipid segregation in PG model membranes, most likely resulting in peptide-depleted and peptide-rich domains, the latter becoming the dominant fraction at high peptide concentrations (Latal et al. 1997). Moreover, this peptide also induced phase separation in liposomes composed of PG/PE, major phospholipid components of bacterial cytoplasmic membranes (Lohner and Prenner 1999). Finally, solid-state NMR measurements (Bechinger et al. 1998), as well as ^{2}H NMR measurements (Wieprecht et al. 2000), are consistent with an orientation of the helical axis of PGLa parallel to the plane of the bilayer. Therefore, we performed X-ray reflectivity and grazing incidence diffraction experiments to study the effect of PGLa on phospholipid monolayers composed of PG and PC, as these techniques provide information on the in-plane structure of the lipid/peptide monolayer, i.e. the in-plane molecular packing. An understanding of how antimicrobial peptides interact with these phospholipids, that are representative for bacterial and mammalian cell membranes, will be helpful for the rational design of novel peptide antibiotics which can selectively kill bacteria.

Materials and methods

Materials

Egg-SM, dipalmitoyl- and distearoylphosphatidylglycerol (DPPG and DSPG) as well as dipalmitoyl- and distearoylphosphatidylcholine (DPPC and DSPC) were obtained from either Sigma (France) or Avanti Polar Lipids (Alabaster, Ala., USA) (purity >99%) and used without further purification. PGLa, consisting of 21 amino acids [GMASKAGAIAGKIAKVALKAL-carboxamide (Andreu et al. 1985)], was purchased from Multiple Peptide Systems (San Diego, Calif., USA). Organic solvents (chloroform, methanol) were of HPLC grade purchased from Sigma (France).

Monolayer experiments

Surface pressure-area (π-A) isotherms were recorded using a custom-designed rectangular Teflon trough with an area of 450×110 mm^2 (MDT Nanotechnology, Moscow, Russia), thermostated at 20 °C. The monolayer was compressed by two moveable Teflon barriers with a velocity of 50 mm/min at surface pressures below 1 mN/m and of 20 mm/min above this value. A Wilhelmy balance with 10 mm wide filter paper was used to measure the surface pressure (π) with an accuracy $\pm$0.1 mN/m. The surface potential (ΔV) was measured with the vibrating capacity method according to Kelvin (Adamson 1982). The vibrating electrode used in the experiment had a disk shape with a diameter of 10 mm. The measured ΔV values are given by the difference of the potential of the monolayer and the potential of the pure water surface, with an experimental error of $\pm$10 mV.

The surface of the subphase was carefully cleaned before each experiment and checked by measuring the surface pressure upon compression, whereby the residual surface pressure was less than 0.2 mN/m at standard conditions of the experiment. The monolayers were prepared by spreading a defined volume of the respective pure component or mixtures of peptides with lipids onto the aqueous subphase (10 mM Na-phosphate, pH 7.4) using a Hamilton syringe. Stock solutions of DPPG and DSPG were prepared in chloroform/methanol (99/1, vol/vol) and of DPPC, DSPC and PGLa in chloroform/methanol (2/1, vol/vol) at a concentration of 1 or 2 mg/mL. After deposition of the samples the monolayer film was equilibrated for at least 1 min before compression in order to ensure evaporation of the organic solvent. All isotherms were measured at least three times.

X-ray techniques

A second Langmuir trough, especially designed for the X-ray experiments, was equipped with a moveable single barrier. The

surface pressure was measured using a Wilhelmy balance with a 3 mm wide filter paper and was kept constant during the measurement. The vessel containing the trough was sealed and filled with a flow of water-saturated helium to reduce evaporation from the subphase interface and parasitic scattering from the air. The compression speed used for the film preparation was the same as for the monolayer studies described above. All X-ray measurements were performed at 20 °C.

Grazing incidence X-ray diffraction (GID) experiments (Als-Nielson et al. 1994) and X-ray reflectivity measurements (XR) (Daillant and Gibaud 1999 and references therein) were performed at the open undulator beamline ID10B at ESRF, Grenoble, France (for details, see http://www.esrf.fr/exp_facilities/ID10B/handbook/). Briefly, a monochromatic synchrotron beam was achieved by using the Bragg reflection from two diamond (111) crystals. The first crystal selects the required wavelength of the "white" X-ray beam coming from the undulator. Both incoming and reflected beams lay in the horizontal plane. The second crystal working in the regime of the symmetric reflection deflected the monochromatic beam back to the initial direction. A system of two platinum mirrors with surfaces in the horizontal plane was used to cut off higher harmonics. The downstream mirror was used to keep the beam in the horizontal plane or to deflect it from the horizontal plane.

In order to perform GID measurements the downstream mirror was used to set the angle of incidence α_i onto the air/water interface at $\alpha_i = 0.85\alpha_c$, where α_c is the critical angle for total external reflection [$\alpha_c = 2.68$ mrad for the wavelength used ($\lambda = 0.155$ nm)]. The diffracted beam was detected by a linear position-sensitive detector (PSD) (PSD-50 M, Braun, Garching, Germany) that records an intensity profile as a function of the vertical scattering angle α_f (Fig. 1a). A Soller collimator in front of the PSD provided a resolution of 0.08° [full width at half maximum (FWHM)] or 0.06 nm^{-1} for the horizontal scattering angle $2\theta_{hor}$. The scattering vector $\boldsymbol{Q}$ (Fig. 1) can be decomposed into two orthogonal components ($\boldsymbol{Q}_{xy}$ and $\boldsymbol{Q}_z$) and is given by:

$$Q^2 = Q_{xy}^2 + Q_z^2 \quad (1)$$

where the vector $\boldsymbol{Q}_{xy} = (4\pi/\lambda)\sin(2\theta_{hor}/2)$ is parallel to the water surface, while the vector $\boldsymbol{Q}_z = (2\pi/\lambda)\sin(\alpha_f)$ is normal to the water surface (Helm et al. 1991). $\boldsymbol{Q}_{xy}$, representing the in-plane component, gives information on the periodic structure of the monolayer parallel to the aqueous subphase, whereas $\boldsymbol{Q}_z$, the out-of-plane component, gives information on the tilt angle and tilt direction of the hydrophobic side chains of the lipids. Furthermore, a peak on an intensity spectrum $I = f(\boldsymbol{Q}_{xy})$, integrated over the whole $\boldsymbol{Q}_z$ range, is defined as a Bragg peak, whereas spectra $I = f(\boldsymbol{Q}_z)$ at a fixed $\boldsymbol{Q}_{xy}$ position are defined as Bragg rods, which were recorded only for $\boldsymbol{Q}_z < 3.5$ nm^{-1} with a vertical resolution of 0.02 nm^{-1} FWHM. The shape of the Bragg peaks and Bragg rods were least-squares fit of a Lorentzian (Durbin et al. 1994), representing the molecules as a cylinder (Porod 1982; Als-Nielson and Kjaer 1989).

The X-ray reflectivity measurements were performed at $\lambda = 0.13838$ nm, where the incident beam was directed on the sample at a glancing incidence angle, α_i. Because of the critical angle of total reflection for platinum ($\alpha_c = 0.42°$), the downstream mirror cannot provide deflection of the beam from the horizontal plane in the angular range required for the reflectivity measurements ($\alpha_i < 5°$). Therefore, the beam coming horizontally after the downstream mirror was deflected downwards by a Ge crystal to a desired angle of incidence α_i with respect to the horizontal liquid surface (Fig. 1b). The crystal that stayed in the Bragg condition for the Ge(111) planes was rotated around the incident beam in a mode such that it always fulfilled the Bragg condition (Fig. 1b). Rotation of the crystal provided the tilt of the diffracted beam and consequently the angle of incidence onto the liquid surface. In such an approach the diffracted beam moves on the surface of a cone. The vertex of the cone is at the deflecting crystal, which results in the incident beam changing its position both in vertical and horizontal directions during the crystal rotation. In order to compensate

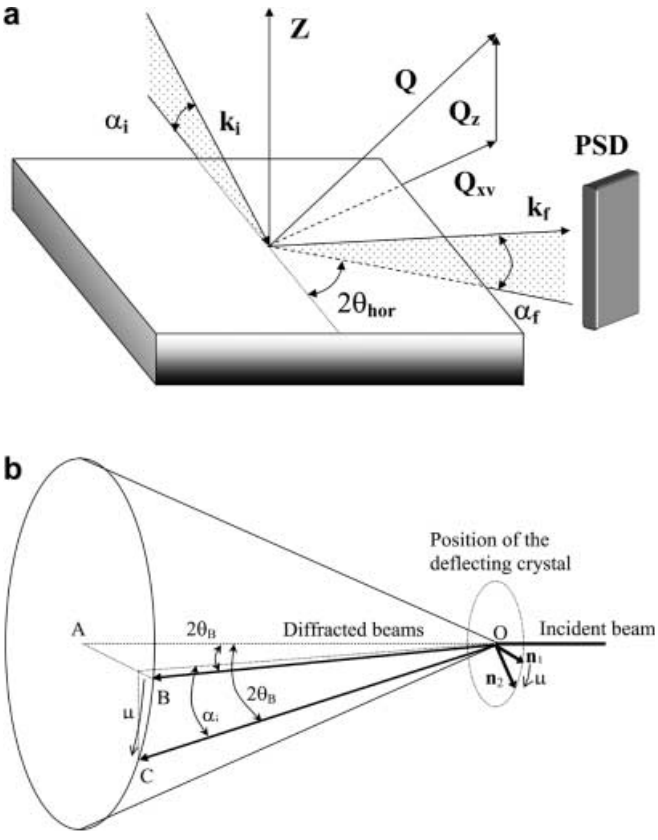

Fig. 1. Scheme of the geometry of X-ray grazing incidence diffraction (**a**) and reflectivity (**b**) from a liquid interface. In GID experiments, α_i is the angle of incidence and α_f the vertical scattering angle, $k_{i,f}$ indicate the respective X-ray beams and the vectors $\boldsymbol{Q}$ are as defined in the text. In reflectivity measurements, OAB defines the horizontal plane, OB, OC are the beams diffracted from the deflecting crystal and n_1, n_2 are the normals to the surface of the deflecting crystal and atomic planes. The vectors OB and n_1 lie in the horizontal plane. θ_B is the Bragg angle and μ is the angle of rotation of the crystal around the incident beam. PSD is the position-sensitive detector

changes of the beam position on the sample plane, the goniometer together with the Langmuir trough were moved in both directions to have the beam footprint at the same location on the sample surface at any incidence angle. The scattering from the interface beam was again detected by a PSD, which allows measurement of both the specular and off-specular signals at the same time. The spectrum obtained at each given incidence angle was fitted by a function composed from a Gaussian and a linear slope, whereby the area under the Gaussian correlates to the reflective intensity. This method allows us to subtract the diffuse scattered component from a spectrum and thereby to gain a background-free reflectivity curve that provides information on the surface-normal electron density profile. This scattering length density (SLD) profile of a film at each experimental condition was reconstructed after the fit of the reflectivity curve with the program REFLAN (Samoilenko et al. 1999). An advantage of REFLAN is that the fitting procedure of the program uses elements of global minimization. This program calculates the reflectivity based on the optics matrix method (Azzam and Bashara 1986), where the whole film is modeled by a stack of homogeneous slabs. Each slab is characterized by its thickness, scattering length density and roughness of the interface. Therefore, the SLD profile of the whole film is a step function. One step of the function is often called a box and hence the total profile is also referred to as the box model.

Results and discussion

Surface pressure/potential-area isotherms

Surface pressure-area (π-A) isotherms of the pure phospholipids are shown in Fig. 2. Both lipids exhibit a point of inflection at a lateral pressure (π_c) of about 10 mN/m for DPPC and 11 mN/m for DPPG, followed by a distinctive plateau region. Such behavior is indicative of a first-order transition from the liquid-expanded to the liquid-condensed state. Both phospholipid films are stable up to 60 mN/m and the surface potential of DPPG was found to be higher by about 200 mV as compared to DPPC (Fig. 2). The surface potentials for both lipids show changes in slope overlapping with the plateau region, i.e. the coexistence range between the liquid-expanded and liquid-condensed state. Finally, all isotherms exhibited a surface pressure less than 0.2 mN/m at areas larger than 2 nm^2/molecule. Furthermore, the surface potential in this area-range had a strong tendency to fluctuate, especially upon mechanical agitation of the water surface. These observations are characteristic for a phospholipid monolayer in a vapor state with clusters of phospholipids at the air/water interface, which suggests a distribution of the material in the form of large islands comparable to the diameter (1 cm) of the vibrating electrode.

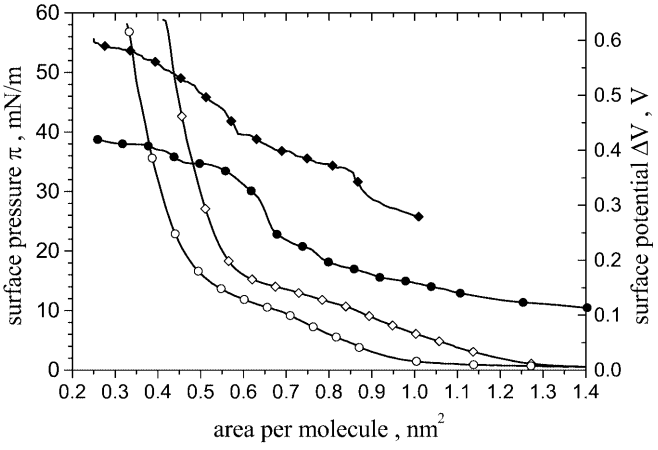

Fig. 2. Surface pressure (*open symbols*) and surface potential (*filled symbols*) isotherms as a function of the molecular area of DPPC (*circles*) and DPPG (*diamonds*), respectively. Measurements were performed at 20 °C; the aqueous subphase was 10 mM Na-phosphate, pH 7.4. Here, and on the following figures, symbols are not all experimental data points; they are used only to differentiate curves

The antimicrobial frog skin peptide PGLa is soluble in water, but owing to the amphipathic character it can be expected that the peptide will form a monolayer at the air/water interface. Therefore, in order to test its surface activity, we spread the peptide solution on the same subphase as used in the lipid experiments. In fact, PGLa formed a very stable monolayer with excellent reproducibility, exhibiting a collapse pressure of about 22 mN/m (Fig. 3). The PGLa monolayer near the point of collapse seems to be still in a liquid phase, as no inclining of the Wilhelmy plate filament from the vertical is observed even at fast and anisotropic compression rates, as can be observed for a solid phase. The surface potential isotherms were also highly reproducible and showed two points of change in slope, one around 8 nm^2/molecule and another one at 5 nm^2/molecule (Fig. 3). In contrast to the phospholipids, the surface potential was stable also at a very low surface pressure (surface area > 10 nm^2/molecule) and when the water subphase was mechanically agitated. Furthermore, in this area range the surface pressure exhibited already a value near 1 mN/m, which is indicative for a gas phase. Provided that the isotherms have been measured with high accuracy, these data can be analyzed according to the equation of the two-dimensional gas state:

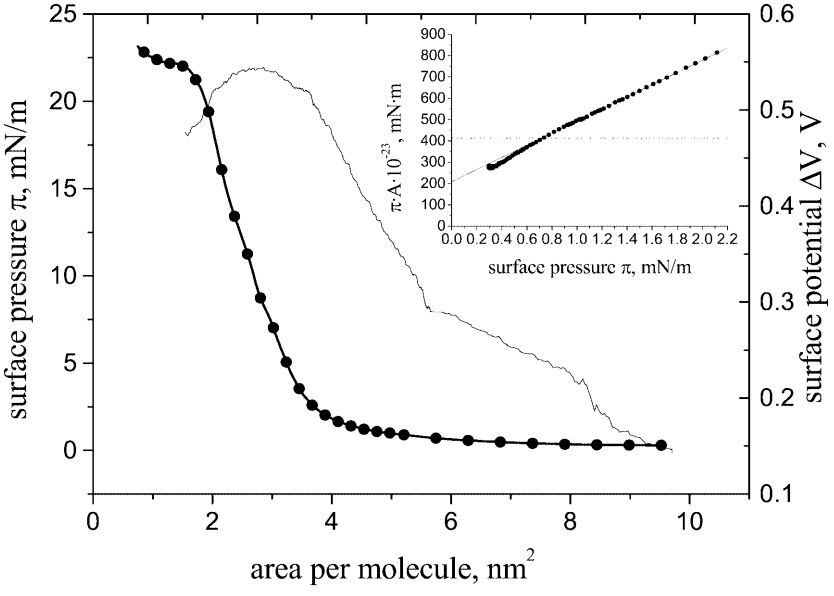

Fig. 3. Surface pressure (*circles*) and surface potential (*line*) isotherms as a function of the molecular area of PGLa at 20 °C; aqueous subphase: 10 mM Na-phosphate, pH 7.4. The *inset* shows the plot (πA versus π) derived from the equation of the two-dimensional gas state to determine A_0 from the slope and the number of peptide molecules in one kinetic unit (for details, see text)

$$\pi(A - A_0) = kT/n \quad (2)$$

where π is the surface pressure, A is the area per one molecule in the monolayer, A_0 is the effective area of collision of the molecule in the monolayer, k is the Boltzmann constant, T is the absolute temperature and n is the average statistical number of molecules in one kinetic unit. Simple transformation yields the linear equation:

$$\pi A = \pi A_0 + kT/n \quad (3)$$

This allows to analyze the π-A isotherms at very low surface pressure in the coordinates of πA versus π, which is shown in Fig. 3 (inset). The linearity of the plot confirms the suitability of this approach. From the slope of this plot a value for A_0 of about 3.4 nm^2/PGLa molecule was calculated. This area would be consistent with the formation of an α-helix at the air/water interface, adopting an orientation of the helical axis parallel to the interface, as shown by the X-ray reflectivity measurements (see below). Assuming an ideal helix (3.6 amino acids/turn and 0.54 nm advance/turn) would yield for PGLa, consisting of 21 amino acids, a length of about 3.1 nm. Taking into account the average helical diameter of about 1.1 nm would result in a molecular area of around 3.4 nm^2. Extrapolation of the plot to zero surface pressure ($\pi \rightarrow 0$) gives $kT/n \approx (215 \pm 15) \times 10^{-23}$ mN m. For $n = 1$, i.e. no association of the molecules, then $kT/n = 413 \times 10^{-23}$ mN m at the experimental temperature of 20 °C. Therefore, a molecular association of two PGLa molecules in one kinetic unit can be estimated under our experimental conditions.

The π-A isotherm for DPPC in the presence of PGLa was characterized by two points of inflection, around 10 mN/m and at 20 mN/m, respectively. The latter one is followed by a distinctive plateau region around 22 mN/m and a further steep increase of the surface pressure upon compression (Fig. 4). The change of slope in the isotherm at higher surface pressure is obviously due to the collapse of the peptide, while the one at lower surface pressure corresponds to the phase change of DPPC from the liquid-expanded to the liquid-condensed state. Furthermore, at large areas the surface pressure is close to the value of ~1 mN/m found for pure PGLa monolayers and the surface potential is stable, even when the barriers are at the outermost position, as observed for the peptide monolayer. The same behavior was found for monolayers composed of PGLa and SM (Fig. 4), another major phospholipid component of eukaryotic cell membranes. These observations clearly indicate that PGLa does not mix on a molecular level with the zwitterionic choline phospholipids, but rather forms islands of peptide clusters in such monolayers. In contrast to the choline phospholipids, the isotherm recorded for the mixture composed of PGLa and the negatively charged DPPG differs completely from the isotherms obtained from the individual components (Fig. 4). First of all, the typical point of collapse for a PGLa monolayer around 22 mN/m cannot be detected, but the

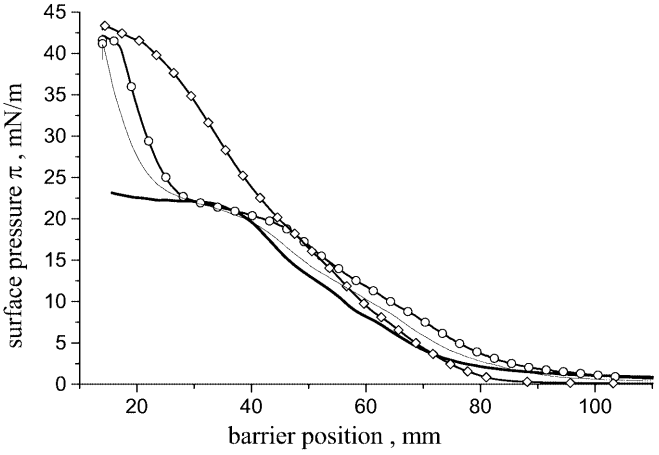

Fig. 4. Surface pressure isotherms as a barrier position of monolayers composed of pure PGLa (*thick line*), binary mixtures of PGLa with DPPC (*circles*), SM (*thin line*) and DPPG (*diamonds*) (1:1 wt/wt). The same total dose (15 μg) of total substance was spread onto the aqueous subphase (10 mM Na-phosphate, pH 7.4) for each experiment. Temperature 20 °C

monolayer now exhibits a collapse pressure slightly higher than 40 mN/m. At large molecular areas the isotherm resembles the features observed in the presence of pure phospholipid films, i.e. the surface pressure is around 0.1 mN/m and the surface potential is unstable, which is consistent with a mixing of the two components at a molecular level. Finally, the surface pressure-area isotherms of lipid monolayers (pure and mixed with peptide) composed of DSPC or DSPG show the same characteristic behavior as observed for DPPC or DPPG. In summary, analyzing (1) the point of collapse, (2) the surface pressure at large areas of the monolayers, i.e. below surface pressures of 1 mN/m, and (3) the stability of the surface potential in this pressure range, we can conclude that the interaction of PGLa with phospholipids can be grouped into one of formation of separate islands of lipids and peptide when zwitterionic phospholipids (DPPC, DSPC, SM) are present, and into one of mixing at a molecular level in the presence of the negatively charged phospholipids (DPPG, DSPG).

Grazing incidence diffraction and X-ray reflectivity experiments

Monolayers of pure components

For GID experiments the film was compressed step-by-step, and the Bragg peaks were recorded at each surface pressure step ($\pi = 15$, 20, 25, 30, 35 and 40 mN/m for lipid monolayers and $\pi = 15$, 22, 27 mN/m for the PGLa monolayer). No measurements could be performed below $\pi < 15$ mN/m because of the weak intensity of the Bragg rods. Furthermore, the GID experiments revealed that the intensity of the Bragg peaks from DPPC and DPPG monolayers was weak compared to DSPC and DSPG. Therefore, owing to the marked difference in

peak intensity, experiments in the presence of the peptide were only performed with the longer chain phospholipids. Nevertheless, the Bragg peak position, as well as its width, of the four phospholipids as a function of surface pressure is presented in Table 1. Our data obtained for monolayers of DPPC and DSPC are in agreement with earlier studies on the variation of the structure as a function of surface pressure (Brezesinski et al. 1995; Struth 1996), although for DPPC monolayers it was shown that such experiments can yield poorly reproducible structural data (personal communication, B. Struth). Two types of Bragg rods were also detected in our experiments, whereby the maximum of the Bragg rods $<10>$ and $<01>$ exhibited a peak at $Q_z \approx 7$ nm^{-1}, while the Bragg rod $<11>$ had a peak at $Q_z = 0$ nm^{-1} and extended on the range $Q_z < 3$ nm^{-1}. The present work focuses, however, on the behavior of the Bragg rod $<11>$, while a detailed analysis of the lattice modification as well as position of the Bragg rods $<10>$ and $<01>$ on Q_z and Q_{xy} axes at different surface pressures and peptide concentrations will be described elsewhere.

In contrast to PC, no structural characteristics of DPPG and DSPG monolayers at the air/water interface have been published yet. The Bragg peak positions for all measured lipids exhibit a linear-like dependence in the applied range of surface pressure (Table 1). It is remarkable that the FWHM of the Bragg peaks remained almost constant over the measured surface pressure range. In general, it has the same value for PG and PC of identical chain length and decreases with increasing chain length. As the obtained values of FWHM are close to the resolution limit of the experimental condition, we were only able to estimate the lower size limit of the 2D powder crystallites being around 60 nm. Analysis of the position of the Bragg peak $<11>$ for the lipid monolayers indicated that the PG monolayer has a larger compressibility than the PC monolayer. The difference in compressibility of the PG and PC lipids can be explained by the difference in the effective size of their polar headgroups. Although these groups cannot be directly seen in GID measurements, as they do not produce a 2D ordering, conclusions about the organization of the lipids can be derived from the ordering of the aliphatic chains that give rise to the Bragg rods. The headgroup of PCs is zwitterionic and packing of the molecules is defined mainly by the physical radius of the molecule, whereas the headgroup of PGs is negatively charged and, hence, the effective radius of these molecules is enlarged owing to electrostatic repulsion. In case of PC lipids, the molecules are already tightly packed and therefore have only a limited possibility, namely by decreasing the hydrocarbon chain tilt, to change the lattice parameters upon compression, while PGs have additional possibilities to reduce the distance between the molecules. This is in agreement with the π-A isotherms of the pure phospholipids (Fig. 2) that show a larger molecular area for PG lipids. Moreover, with increasing surface pressure the Bragg peak $<11>$ shifts to higher Q_{xy} values for all lipids measured (Fig. 5), indicating that the molecular distance in the film plane decreases. This can be attributed to a decrease of the tilt angle of the aliphatic chains for both PG and PC. In accordance with this observation, reflectivity measurements, shown for example for DSPG (Fig. 6), demonstrate that upon compression the monolayer thickness increases (Table 2). This fact was already reported earlier for the DPPC monolayer (Thoma et al. 1996). It should be mentioned that this parameter can be determined accurately, whereas there exists some uncertainty to calculate reliable tilt angles of the hydrocarbon chains in a separate determination of the thicknesses of the headgroup and hydrocarbon layer at low surface pressures (for DSPG and DSPC, below 15 mN/m).

The GID spectrum of the peptide monolayer was measured in a wide Q_{xy} range (4–29 nm^{-1}) and did not show any Bragg peak at all surface pressures applied (data not shown). The spectra are smooth curves that decreased monotonically with an increase of Q_{xy} following the law $1/Q_{xy}^2$, owing to capillary waves at the surface (Fradin et al. 2000). This suggests that peptide-dimer formation, estimated from the π-A isotherm, does not lead to self-aggregation with subsequent crystallite formation.

The X-ray reflectivity measurements of the PGLa monolayer show negligible variation of the vertical structure of the film upon increase of the surface pressure below the collapse point ($\sim$22 mN/m), but differ above it (Fig. 7). Analysis by the standard one-box model gave a reasonable fit of the reflectivity data for the PGLa monolayer, but was difficult to be interpreted on a physicochemical basis. The best fit yielded a layer thickness of 0.56 nm, a small roughness of the air/film interface but a strong roughness of the water/film interface of 1.5 nm. The roughness in such an analysis characterizes the width of the interface where the

Table 1. In-plane Bragg peak position ($Q_{xy<11>}$) and peak width [$\Delta Q_{xy<11>}$ (FWHM)] for PC, PG and mixed PGLa/DSPC (1/1 wt/wt) monolayers at different surface pressures (π)

π (mN/m)	$Q_{xy<11>}$ (nm^{-1})					$\Delta Q_{xy<11>}$ (nm^{-1})				
	DPPG	DPPC	DSPG	DSPC	DSPC/PGLa	DPPG	DPPC	DSPG	DSPC	DSPC/PGLa
15	14.64	14.59	14.54	14.53	14.54	0.14	0.15	0.08	0.10	0.11
20	14.70	14.66	14.59	14.54	14.57	0.13	0.12	0.09	0.08	0.08
25	14.74	14.67	14.63	14.59	14.60	0.11	0.15	0.08	0.09	0.10
30	14.79	14.67	14.68	14.61	14.63	0.11	0.11	0.09	0.09	0.10
35	14.83	14.70	14.73	14.63	14.65	0.10	0.12	0.08	0.10	0.10
40	14.88	14.72	14.79	14.66	–	0.14	0.14	0.09	0.10	–

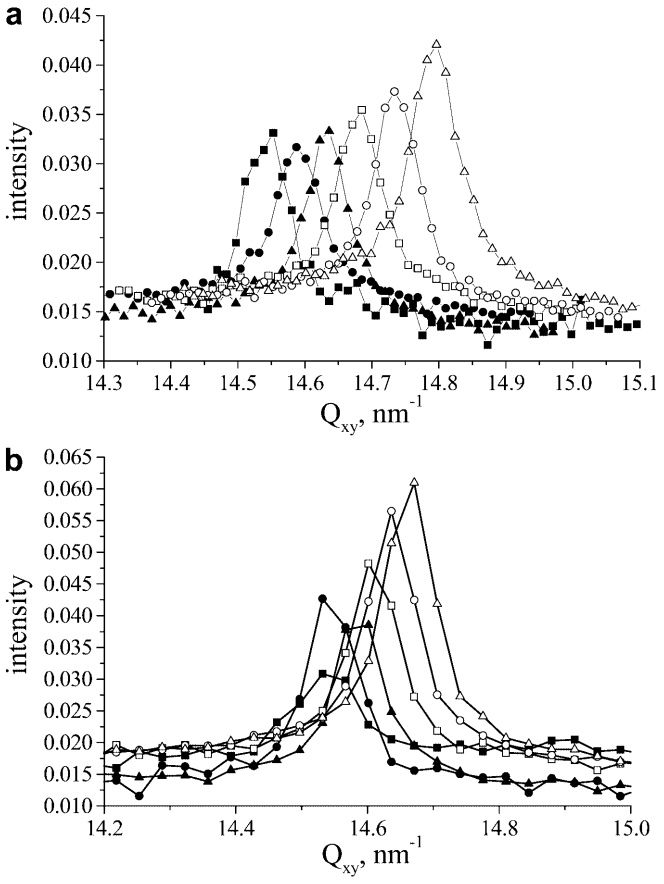

Fig. 5. Measured GID at $Q_z = 0$ for DSPG (**a**) and DSPC (**b**) monolayers at different surface pressures: 15 mN/m (*filled squares*), 20 mN/m (*filled circles*), 25 mN/m (*filled triangles*), 30 mN/m (*open squares*), 35 mN/m (*open circles*), 40 mN/m (*open triangles*); aqueous subphase of 10 mM Na-phosphate, pH 7.4

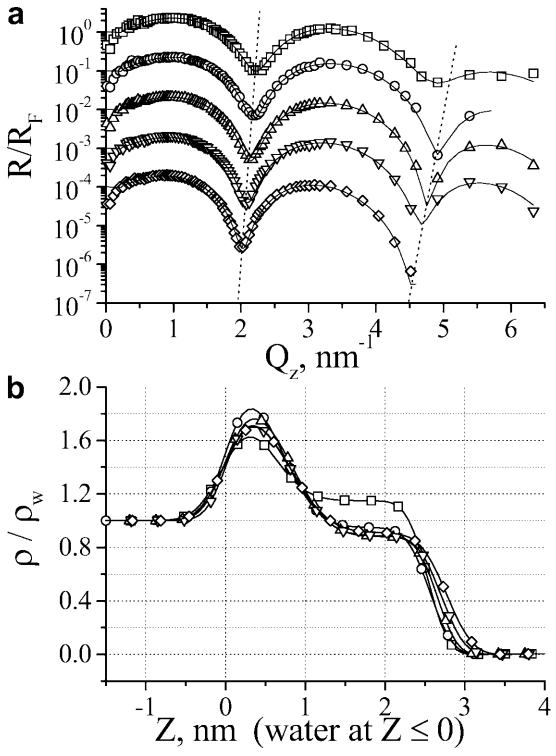

Fig. 6. Measured points (*symbols*) and fitted (*lines*) Fresnel normalized X-ray reflectivities of a DSPG monolayer (**a**) at different surface pressures: 10 mN/m (*squares*), 15 mN/m (*circles*), 20 mN/m (*up triangles*), 30 mN/m (*down triangles*), 40 mN/m (*diamonds*); aqueous subphase of 10 mM Na-phosphate, pH 7.4. For clarity, the number of points on the experimental curves were reduced by a factor of 3. The corresponding scattering length density profiles are shown in (**b**). Symbols are as in (**a**); the aqueous subphase corresponds to $Z \leq 0$

scattering length density profile monotonously changes from a SLD of the water (SLD_W) to a SLD of the layer. Hence, it is obviously difficult to build a physically reasonable SLD profile based on the fact that the roughness is three times larger than the layer thickness. Therefore, we used another model to fit the reflectivity data of the peptide monolayer. This model takes into account a smooth variation of the SLD profile on a large length. The new model of the SLD profile (SLD_P) was inspired by the results of fitting the data with the box model and is composed by two error-like functions that are usually used to describe a density variation at the interface of two media in reflectivity experiments (Als-Nielsen and Kjær 1989):

$$\mathrm{SLD_P}(z) = \begin{cases} f_1 = \mathrm{SLD_W} + (A - \mathrm{SLD_W})/(1 + \exp(-z)/\sigma_2), & ;z \leq 0 \\ f_3 = \min(f_1, f_2), & 0 < z < Z_0 \\ f_2 = A/(1 + \exp(z - Z_0)/\sigma_1), & z \geq Z_0 \end{cases} \quad (4)$$

where SLD_W is the scattering density of the water, σ_1 and σ_2 the roughness of the air/film and film/water interface, respectively, A is the maximum of the SLD value in the layer, and Z_0 the distance between the centers of the two functions and represents the layer thickness. Because of its simplicity, we used the exponential function instead of the true error function. This kind of model for the SLD profile has the same number of fitting

Table 2. Structural parameters of DSPG and DSPC monolayers as a function of surface pressure (π) derived from X-ray reflectivity data

Lipid	π (mN/m)	Thickness of headgroup, l_{hg} (nm)	Thickness of hydrocarbon layer, l_{hc} (nm)	Total thickness, $l_{hg} + l_{hc}$ (nm)
DSPG	15	0.718	1.856	2.574
	20	0.847	1.817	2.664
	30	0.845	1.873	2.718
	40	0.800	1.985	2.785
DSPC	15	1.230	1.474	2.704

parameters (four) as the one-box model. Using this model, a thickness of the peptide layer of about 0.8 nm was calculated, characterized by a sharp air/peptide interface and a very smooth peptide/water interface (Fig. 7b). The calculated layer thickness indicates a parallel orientation of the axis of the peptide to the water surface, which can be expected from the distribution of the charged/polar and hydrophobic amino acids along the PGLa molecule, and is in agreement with results from NMR measurements (Bechinger et al. 1998; Wieprecht et al. 2000).

Monolayers of binary mixtures

The GID data obtained from monolayers of PGLa and DSPC mixtures showed the same features as observed for the monolayer of pure DSPC at the corresponding surface pressure and can be considered as the sum of the two spectra of the pure substances. Neither the Bragg peak position nor its FWHM were affected by the presence of the peptide (Table 1). This observation suggests that the peptide molecules do not incorporate into the 2D lattice of the PC lipids and, hence, do not change the size of the crystallites. The film thicknesses of the lipid layers, calculated from Bragg rods corresponding to the Bragg peak from the DSPC crystallites, are the same as for the pure components. Comparisons of the width of the Bragg peak ($\Delta \boldsymbol{Q}_{xy}$) (Table 1) do not show distinct changes in the size of the crystallites of the peptide and of DSPC in the mixture. However, the Bragg peak intensity of the mixed layer is smaller than the intensity of the layer of pure DSPC, which is due to the dilution of the number of lipid crystallites in the area illuminated by the X-ray beam. The SLD profile reconstructed from the reflectivity curve of the mixed monolayer (Fig. 8) is in agreement with a two-phase system in the film. The layers of the lipid headgroups and of the peptide have roughly the same density, thickness and location at the air/water interface. Therefore, the corresponding box model for the mixed layer shows no change in the thickness and density when compared with the same parameters of the pure lipid film. In contrast, the density of the box corresponding to the location of the aliphatic chains is now a mean value of the densities of closely packed islands of the aliphatic chains and the "holes" arising from the peptide. Such an averaging does not change the box thickness but does

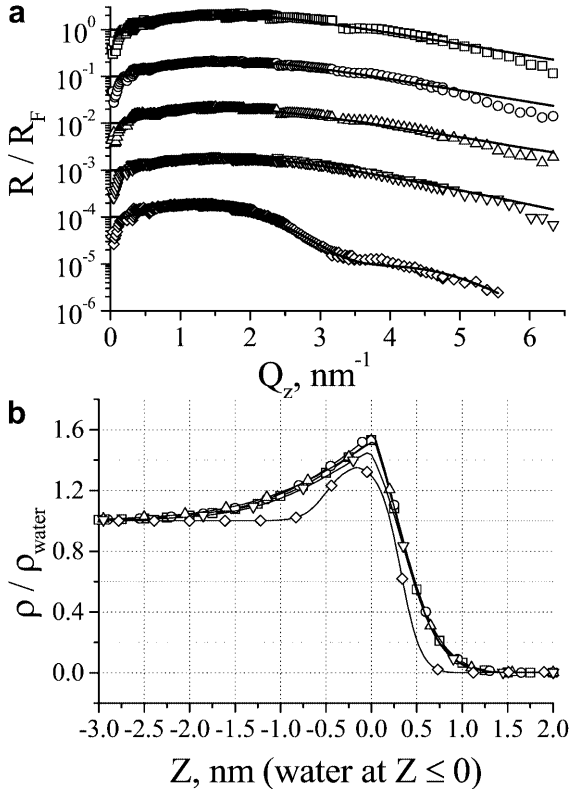

Fig. 7. Measured points (*symbols*) and fitted (*lines*) Fresnel normalized X-ray reflectivities of a PGLa monolayer (**a**) at different surface pressures: 5 mN/m (*squares*), 10 mN/m (*circles*), 15 mN/m (*up triangles*), 20 mN/m (*down triangles*), 25 mN/m (*diamonds*); aqueous subphase of 10 mM Na-phosphate, pH 7.4. For clarity, the number of points on the experimental curves were reduced by a factor of 3. The corresponding scattering length density profiles are shown in (**b**). Symbols are as in (**a**); the aqueous subphase corresponds to $Z \leq 0$

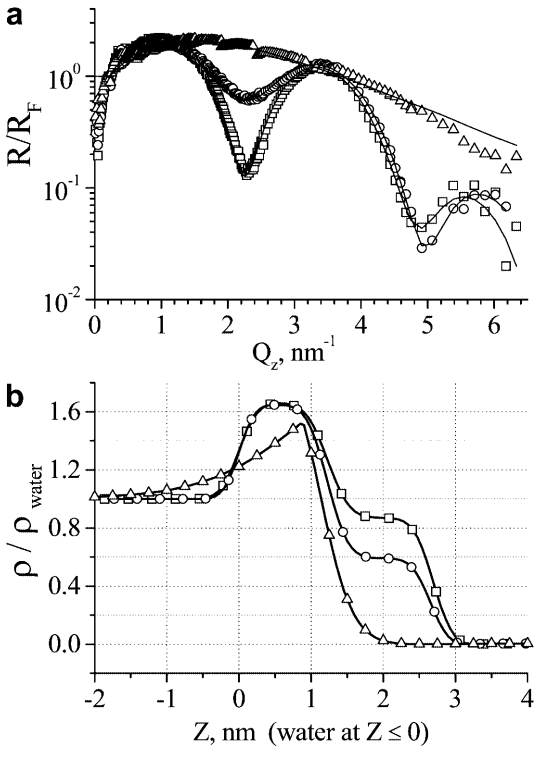

Fig. 8. Measured points (*symbols*) and fitted (*lines*) Fresnel normalized X-ray reflectivities of monolayers consisting of DSPC (*squares*), PGLa (*triangles*) and a mixture of DSPC/PGLa (1:1 wt/wt) (*circles*) at a surface pressure of 15 mN/m; aqueous subphase of 10 mM Na-phosphate, pH 7.4. For clarity, the number of points on the experimental curves were reduced by a factor of 3. The corresponding scattering length density profiles are shown in (**b**). Symbols are as in (**a**); the aqueous subphase corresponds to $Z \leq 0$

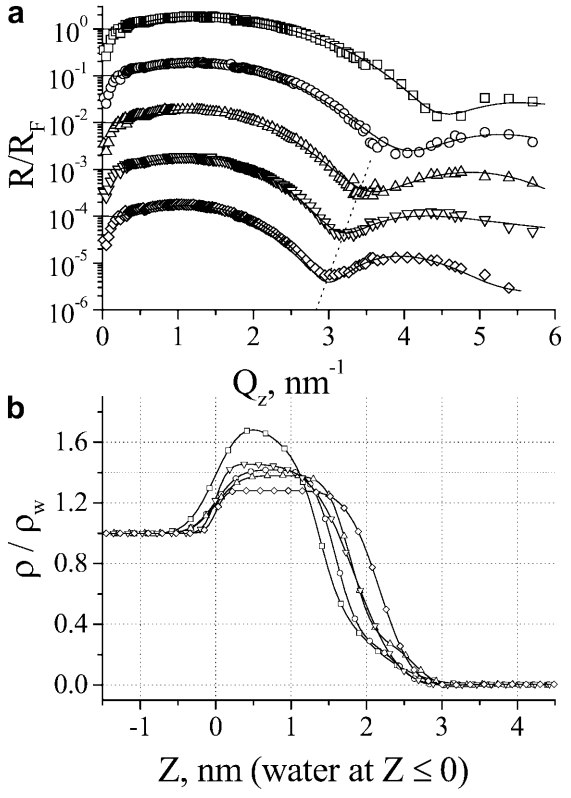

Fig. 9. Measured points (*symbols*) and fitted (*lines*) Fresnel normalized X-ray reflectivities of a DSPG/PGLa (1:1 wt/wt) monolayer (**a**) at different surface pressures: 5 mN/m (*squares*), 10 mN/m (*circles*), 15 mN/m (*up triangles*), 20 mN/m (*down triangles*), 25 mN/m (*diamonds*); aqueous subphase of 10 mM Na-phosphate, pH 7.4. For clarity, the number of points on the experimental curves were reduced by a factor of 3. The corresponding scattering length density profiles are shown in (**b**). Symbols are as in (**a**); the aqueous subphase corresponds to $Z \leq 0$

reduce the density. Exactly this is observed from the SLD profile of the mixed DSPC + PGLa monolayer (Fig. 8b). Provided that the lipids do not form islands, the distance between the lipid molecules would increase, thereby leading to an increase of the tilt angle of the molecules and as a consequence to a decrease of the layer thickness. This would induce a dramatic change in the Bragg peak position, which was not observed in our experiment. Therefore, both GID and XR clearly indicate that PGLa does not mix at a molecular level with the zwitterionic phospholipids, supporting the conclusions from the surface-pressure area isotherms and earlier DSC data (Latal et al. 1997). Interestingly, the first GID study on highly oriented multilamellar lipid-peptide samples showed that an antimicrobial peptide, magainin 2, strongly perturbs the ordering of the aliphatic chains of DMPC (Munster et al. 2000). This may indicate a different mechanism of action of the peptides, but more likely may be due to different experimental conditions, such as, for example, hydration of the lipids.

However, the GID spectrum obtained for PGLa and DSPG mixtures is similar to the one for pure PGLa and is obviously not the sum of the spectra of the pure substances (data not shown). No Bragg peaks arising from the crystallites formed by the DSPG molecules were found at all measured surface pressures. This clearly demonstrates that the presence of the peptide destroys the integrity of the layer (chain order) from the phospholipid and demonstrates that the peptide penetrates into the lipid chain region and does not adsorb onto the headgroups, as has been reported from a first GID study on highly aligned multilamellar phospholipid membranes containing the antimicrobial peptide magainin 2 (Munster et al. 2000). Reflectivity measurements (Fig. 9) of the DSPG and PGLa mixture shows that the film thickness increased with increasing surface pressure and that the film is rather homogeneous in terms of SLD variation. An explanation of such behavior is that the cationic peptide molecules insert in-between the negatively charged PG headgroups owing to electrostatic interaction, which will induce a strong tilt or disordering of the aliphatic chains of the lipids in order to maximize the van der Waal's interaction. As a result, the conformational change of the aliphatic chains from *trans* to *gauche* will cause an increase of area per chain. All these reasons can lead to the loss of in-plane order and formation of a lipid-peptide layer with homogeneous properties along the film normal. This observation also supports the suggestion of domain formation in DPPG liposomes upon addition of PGLa, concluded from microcalorimetric studies (Latal et al. 1997), as the negatively charged lipid obviously adopts different structures in the presence and absence of the peptide. Finally, the growth of layer thickness upon increase of surface pressure is explained by a decrease of the tilt angle and/or increase of order of the lipid molecules, when they get in closer contact.

This first synchrotron GID and reflectivity study on phospholipid monolayers at the air/water interface in the presence of the antimicrobial frog skin peptide PGLa demonstrates that the peptide perturbs the order of the negatively charged phosphatidylglycerol lipids, but does not affect the structural organization of the zwitterionic phosphatidylcholine lipids. Moreover, it was shown that PGLa itself does form stable monolayers, but does not exhibit any tendency to form a two-dimensional structure at the air/water interface. The results clearly show that these techniques, which are sensitive to the ordering of molecules on an atomic length scale, are applicable for studying the molecular mechanism of lipid-peptide interactions.

Acknowledgements The authors gratefully acknowledge financial support by the Jubiläumsfonds der Österreichischen Nationalbank (project 5100 to K.L.).

References

Adamson AW (ed) (1982) Physical chemistry of surfaces. Wiley, New York

Als-Nielsen J, Kjær K (1989) X-ray reflectivity and diffraction studies of liquid surfaces and surfactant monolayers. In: Riste T,

Sherrington D (eds) Phase transitions in soft condensed matter. (NATO advanced science institutes series B: physics, vol 211) Plenum, New York, pp 113–138

Als-Nielsen J, Jacquemain D, Kjaer K, Leveiller F, Lahav M, Leiserowitz L (1994) Principles and applications of grazing incidence X-ray and neutron scattering from ordered molecular monolayers at the air-water interface. Phys Rep 246:251–313

Andreu D, Aschauer H, Kreil G, Merrifield RB (1985) Solid-phase synthesis of PYL[a] and isolation of its natural counterpart, PGL[PYL[a]-(4–24)] from skin secretion of *Xenopus laevis*. Eur J Biochem 149:531–535

Azzam RMA, Bashara NM (eds) (1986) Elipsometry and polarized light. North-Holland, Amsterdam

Bechinger B, Zasloff M, Opella SJ (1998) Structure and dynamics of the antibiotic peptide PGLa in membrane by solution and solid state nuclear magnetic resonance spectroscopy. Biophys J 74:981–987

Boman HG (1991) Antibacterial peptides: key components needed in immunity. Cell 65:205–207

Brezesinski G, Dietrich A, Struth B, Böhm C, Bouwman WG, Kjaer K, Möhwald H (1995) Influence of ether linkages on the structure of double-chain phospholipid monolayers. Chem Phys Lipids 76:145–157

Daillant J, Gibaud A (eds) (1999) X-ray and neutron reflectivity: principles and applications. Springer, Berlin Heidelberg New York

Davies J (1996) Bacteria on the rampage. Nature 383:219–220

Durbin MK, Malik A, Ghaskadvi R, Shilh MC, Zschack P, Dutta P (1994) X-ray diffraction study of a recently identified phase transition in fatty acid Langmuir monolayers. J Phys Chem 98:1753–1755

Fradin C, Braslau A, Luzet D, Smilgies D, Alba M, Boudet N, Mecke K, Daillant J (2000) Reduction in the surface energy of liquid interfaces at short length scales. Nature 403:871–874

Ganz T, Lehrer RI (2001) Antimicrobial peptides in innate immunity. In: Lohner K (ed) Development of novel antimicrobial agents: emerging strategies. Horizon Scientific, Wymondham, Norfolk, UK, pp 139–147

Helm CA, Tippmann-Krayer P, Möhwald H, Als-Nielsen J, Kjaer K (1991) Phases of phosphatidylethanolamine monolayers studied by synchrotron X-ray scattering. Biophys J 60:1457–1476

Latal A, Lehrer RI, Harwig, SSL, Lohner K (1996) Interaction of enantiomeric protegrins with liposomes. Prog Biophys Mol Biol 65:121

Latal A, Degovics G, Epand RF, Epand RM, Lohner K (1997) Structural aspects of the interaction of PGLa, a highly potent antimicrobial peptide from frog skin, with lipids. Eur J Biochem 248:938–946

Lohner K (2001) The role of membrane lipid composition in cell targeting of antimicrobial peptides. In: Lohner K (ed) Development of novel antimicrobial agents: emerging strategies. Horizon Scientific, Wymondham, Norfolk, UK, pp 149–165

Lohner K, Epand RM (1997) Membrane interactions of hemolytic and antibacterial peptides. In: Bush CA (ed) Advances in biophysical chemistry, vol 6. JAI, Greenwich, Conn., USA, pp 53–66

Lohner K, Prenner EJ (1999) Differential scanning calorimetry and X-ray diffraction studies of the specificity of the interaction of antimicrobial peptides with membrane-mimetic systems. Biochim Biophys Acta 1462:141–156

Lohner K, Staudegger E (2001) Are we on the threshold of the post-antibiotic era? In: Lohner K (ed) Development of novel antimicrobial agents: emerging strategies. Horizon Scientific, Wymondham, Norfolk, UK, pp 1–15

Lohner K, Latal A, Lehrer RI, Ganz T (1997) Differential scanning microcalorimetry indicates that human defensin, HNP-2, interacts specifically with biomembrane mimetic systems. Biochemistry 36:1525–1531

Matsuzaki M, Sugishita K, Harada M, Fujii N, Miyajima K (1997) Interactions of an antimicrobial peptide, magainin 2, with outer and inner membranes of Gram-negative bacteria. Biochim Biophys Acta 1327:119–130

Munster C, Lu J, Bechinger B, Salditt T (2000) Grazing incidence X-ray diffraction of highly aligned phospholipid membranes containing the antimicrobial peptide magainin 2. Eur Biophys J 28:683–688

Nakamura T, Furunaka H, Miyata T, Tokunaga F, Muta T, Iwanaga S, Niwa M, Takao T, Shimonishi Y (1988) Tachyplesin, a class of antimicrobial peptide from the hemocytes of the horseshoe crab (*Tachypleus tridentatus*). Isolation and chemical structure. J Biol Chem 263:16709–16713

Porod G (1982) General theory. In: Glatter O, Kratky O (eds) Small angle X-ray scattering. Academic, London, pp 17–51

Samoilenko II, Konovalov OV, Feigin LA, Shchedrin BM, Yanusova LG (1999) Processing of experimental reflectivity data within the REFLAN software package. Crystallogr Rep 44:310–318

Struth B (1996) Strukturcharakterisierung von Monoschichten und wäßrigen Dispersionen chemisch modifizierter Phospholipide. Thesis, Mainz

Thoma M, Schwendler M, Baltes H, Helm CA, Pfohl T, Riegler H, Möhwald H (1996) Ellipsometry and X-ray reflectivity studies on monolayers of phosphatidylethanolamine and phosphatidylcholine in contact with *n*-dodecane, *n*-hexadecane, and bicyclohexyl. Langmuir 12:1722–1728

Tossi A, Sandri L, Giangaspero A (2000) Amphipathic, α-helical antimicrobial peptides. Biopolymers (Pept Sci) 55:4–30

White SH, Wimley WC, Selsted ME (1995) Structure, function, and membrane integration of defensin. Curr Opin Struct Biol 5:521–527

Wieprecht T, Apostolov O, Beyermann M, Seelig J (2000) Membrane binding and pore formation of the antibacterial peptide PGLa: thermodynamic and mechanistic aspects. Biochemistry 39:442–452